Tunneling into Multiwalled Carbon Nanotubes: Coulomb Blockade and the Fano Resonance

W. Yi,[1,*] L. Lu,[1] H. Hu,[2] Z.W. Pan,[1] and S. S. Xie[1]

[1]*Institute of Physics, Chinese Academy of Sciences, Beijing 100080, People's Republic of China*
[2]*Department of Physics, Tsinghua University, Beijing 100084, People's Republic of China*

(Received 20 March 2003; published 12 August 2003)

Tunneling spectroscopy measurements of single tunnel junctions formed between multiwalled carbon nanotubes (MWNTs) and a normal metal are reported. Intrinsic Coulomb interactions in the MWNTs give rise to a strong zero-bias suppression of a tunneling density of states that can be fitted numerically to the environmental quantum-fluctuation theory. An asymmetric conductance anomaly near zero bias is found at low temperatures and interpreted as Fano resonance in the strong tunneling regime.

DOI: 10.1103/PhysRevLett.91.076801 PACS numbers: 73.63.Fg, 73.23.Hk, 85.35.Kt

Coulomb blockade (CB) has been studied intensively in a multijunction configuration, in which electron tunnel rates from the environment to a capacitively isolated "island" are blocked by the *e-e* interaction if the thermal fluctuation is below the charging energy $E_c = e^2/2C$ and the quantum fluctuation is suppressed with sufficiently large tunnel resistance $R_t \gg R_Q = h/2e^2$. In the case of a single-junction circuit, the understanding of CB is less straightforward. The Coulomb gap, supposedly less significant for the case of low-impedance environments, should be established only if the environmental impedance exceeds R_Q.

In single-walled carbon nanotubes (SWNTs), the reduced geometry gives rise to strong *e-e* interaction. Indeed, CB oscillations and evidence of Luttinger liquid (LL) have been observed [1]. In contrast to SWNTs, in which only two conductance channels are available for current transport, multiwalled carbon nanotubes (MWNTs) with diameter in the range of $d = 20$–40 nm have several tens of conductance channels. The energy separation of the quantized subbands, given by $\Delta E = \hbar v_f/d$, is about 13–26 meV taking the Fermi velocity $v_f = 8 \times 10^5$ m/s. This value is about an order of magnitude smaller than that of SWNTs. Experiments indicate that MWNTs are considerably hole doped, thus a large number of subbands, on the order of 10, are occupied. Observations of weak localization [2], electron phase interference effect [3], and universal conductance fluctuations [2] support the view that low frequency conductance in MWNTs is contributed mostly by the outmost graphene shell and is characterized by 2D diffusive transport. In addition to the phase interference effects, a strong *e-e* interaction has also been observed in MWNTs. Pronounced zero-bias suppression of the tunneling density of states (TDOS) has been observed several times in the tunneling measurements [4–6]. Moreover, the TDOS shows a power law, i.e., $\nu(E) \sim E^{\alpha}$, which resembles the case of a LL. It is noteworthy that in the environmental quantum-fluctuation (EQF) theory, for a single tunnel junction coupled to high-impedance transmission lines, such a scaling behavior is also predicted at the limit of many parallel transmission modes [7]. The physical origin of these power laws is the linear dispersion of bosonic excitations that are characteristic both for LL, which is a strictly 1D ballistic conductor, and a single tunnel junction connected to a 3D disordered conductor. In the latter case, the quasiparticle tunneling is suppressed at $V \ll e/2C$, therefore the charge is transported with 1D plasmon modes. The fact that MWNTs have many conductance modes, together with the observation of a crossover from power law to Ohmic behavior at higher voltages [6], suggests that the EQF theory is more appropriate to describe the observed TDOS renormalization. However, most of these measurements were done in multijunction configurations. A single tunnel junction measurement is needed to further clarify this issue.

In this Letter, millimeter-long chemical vapor deposition grown MWNTs [8] are measured by a cross-junction method. The MWNT samples are composed of loosely entangled nanotubes of diameters between 20 to 40 nm that are roughly parallel to each other and up to 2 mm long. The single tunnel junctions are formed by crossing a very thin (< 1 μm) MWNT bundle with a narrow strip of metal wire fabricated on an insulating substrate. We explored different electrode materials including Au, Cu, Sn, and Al. In the case of Sn and Al, a small magnetic field is applied to suppress the superconducting state below T_c. No obvious change of device characteristics attributable to the choice of metals is observed [9]. With such a cross-junction configuration the measured conductance is contributed exclusively by the tunnel junction, since the current is passed along one arm of the MWNT/metal and the voltage is measured along the other, noncurrent carrying arm. Thus the device can be understood as a small number of single tunnel junctions in parallel. Despite the simplicity of their fabrication, we find that the devices are very stable and sustain several cooling cycles without apparent change of characteristics. More than 20 samples are measured, all yielding strong zero-bias suppression of the TDOS.

The current $I(V)$ and $G \equiv dI/dV$ are calculated by a golden-rule approach incorporating the environmental influence by $P(E)$, the probability for a tunneling electron to lose energy to the environment. $P(E)$ can be calculated

from its Fourier transform, the phase correlation function $J(t)$. In the transmission-line model, $J(t)$ is determined by the total environmental impedance $Z_t(\omega) = [i\omega C + Z^{-1}(\omega)]^{-1}$, where $Z(\omega)$ is the external environmental impedance. We apply the method in Ref. [10] to evaluate $P(E)$ from an integral equation without the need of going to the time domain. The I-V characteristics are then calculated for finite temperatures and arbitrary junction impedance. The parameters that appear in the numerical calculation are the damping strength $\alpha = Z(0)/R_Q$, the inverse relaxation time ω_{RC}, and the quality factor $Q = \omega_{RC}/\omega_S$ with the resonance frequency of the undamped circuit $\omega_S = (LC)^{-1/2}$. It is noted that the quality factor Q plays only a minor role as an additional adjustable parameter. Therefore it is not important to the fit and is always set to unit.

We then try to fit our experimental data with the EQF theory. Since E_c and R_t are determined by the high-voltage data, the isolation resistance $R_{\rm iso} = Z(0)$ is the only adjustable parameter in our fitting. In contrast to the case of Ref. [11], where $R_{\rm iso}$ is formed by ideal Ohmic and temperature-independent resistors, $R_{\rm iso}$ in our case is provided by the resistive impedance of the MWNTs themselves, which should be temperature dependent. Indeed, from the fitting, we see an evolution of α from 0.1 at 20 K to 0.25 at 1–4 K and then α saturates [Fig. 1(c)]. Note that dimensionless units are used with G normalized by $1/R_t$ and voltage normalized by $e/2C$. Therefore the number of the single tunnel junctions has no effect on the fitting, and our measurements of different samples can be directly compared. We find that for different samples with scattered characteristics (see Table I), at low temperatures the exponent α reaches a universal value of 0.25–0.35, which agrees with previous multijunction measurements [5,6]. It yields $R_{\rm iso} =$ 3.3–4.6 kΩ, which is roughly a constant for different samples. This coincidence is not accidental but reflects the intrinsic electrodynamic modes of the MWNTs, which can be modeled as an ideal resistive LC transmission line: $R = (L'/C')^{1/2}$ with the kinetic inductance estimated as $L' = R_Q/2N\upsilon_f \approx 1$ nH/μm for $N \approx 10$–20 modes and the capacitance $C' \approx 20$–30 aF/μm. Therefore, the "environment" with respect to the single junctions in our devices is provided by MWNTs themselves, not by the external circuits.

It is interesting that the exponent α, hence $Z(0)$, saturates at very low temperatures [Fig. 1(c)]. Similar saturation in tube resistance was previously observed by Langer *et al.* [2]. It should reflect the saturation of dephasing time, which is a common phenomenon observed in many mesoscopic systems, but the origin is still in debate [12]. This argument is consistent with our magnetoresistance measurement on the same batch of MWNTs [13]. It would be interesting to examine the specific dephasing mechanism in MWNTs by considering the EQF process.

As mentioned previously, for an isolated single tunnel junction with many parallel transport modes, the EQF theory predicts a power-law asymptotics: $G(V,T)/G(0,T) \equiv f(V/T) = |\Gamma[\frac{1}{2}(\alpha+2) + (ieV/2\pi k_BT)]/\Gamma[\frac{1}{2}(\alpha+2)]\Gamma[1+(ieV/2\pi k_BT)]|^2$, where $G(0,T)$ is the zero-bias conductance, and $\Gamma(x)$ is the gamma function [11]. For $eV/2\pi k_BT \gg 1$, a voltage power law $G(V,T) \sim V^\alpha$ is expected. Note that in the above scaling function, exponent α is the only adjustable parameter. In Fig. 2, we can observe such a scaling behavior. Here $f(V/T)$, represented by the dashed line, is calculated taking $\alpha =$ 0.27. The inset shows the original data in which the dashed line is calculated numerically using the same exponent $\alpha = 0.27$.

CB and Coulomb gap effects in MWNTs are recently described with microscopic theories in Refs. [14,15]. In the 2D diffusive regime, the exponent for tunneling into

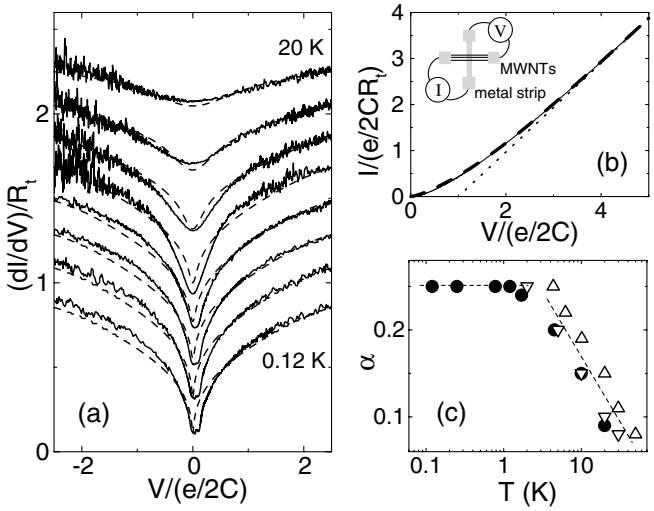

FIG. 1. (a) dI/dV as a function of V in dimensionless units measured at $T = 0.12$, 0.25, 0.78, 1.2, 1.7, 4.5, 10, 20 K (sample 990530s6, curves are offset for clarity). Dashed lines are the fits of EQF theory. (b) Solid line is the dc current simultaneously measured at 0.12 K. Dashed line (right on top of the solid line) is the numerical fit. Dotted line shows a Coulomb offset of $e/2C$ ($e/2C = 10$ mV, $e/2CR_t = 1.16$ μA). The inset illustrates the four-probe configuration of the tunneling conductance measurement between a metal strip and several parallel MWNTs. (c) The temperature dependence of the exponent α for three samples (●: 990530s6; △: 990316; ▽: 990320).

TABLE I. A partial list of characteristics of the samples.

Sample	R_t (kΩ)	E_c (eV)	C (aF)	$R_{\rm iso}$ (kΩ)	α
990316	18.4	0.019	4.2	3.3[a]	0.25[a]
990320	48.3	0.014	5.7	3.3[a]	0.25[a]
990530s6	8.6	0.01	8.0	3.3[a]	0.25[a]
990530s1	10.0	0.02	4.0	4.6[a]	0.35[a]
990202	9.1	0.004	20.0	3.5[a]	0.27[a]

[a]Value acquired at $T = 1.2$–4.3 K.

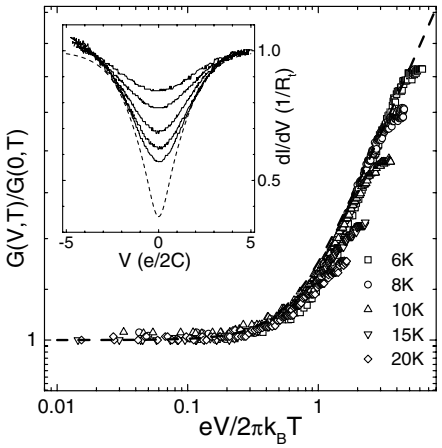

FIG. 2. Scaled conductance $G(V,T)/G(0,T)$ of another sample (990202). The inset shows the original dI/dV vs V. The dashed lines in both frames represent the EQF theory with exponent $\alpha = 0.27$.

the bulk of a MWNT is $\alpha = (R/h\nu_0 D)\ln(1 + \nu_0 U_0)$. Here R is the tube radius, U_0 is the intratube Coulomb interaction, $D = \nu_f^2\tau/2$ is the charge diffusivity, and the "bare" DOS $\nu_0 = N/4h\nu_f$ with $N \approx 20$. If we use $\nu_f\tau \approx$ 60 nm from the magnetoresistance data [13] and taking $R = 20$ nm, then under the condition of $U_0/h\nu_f \sim 1$ the above formula yields $\alpha \approx 0.25$, which agrees with our experiment.

Besides the voltage power-law phenomenon, which is characteristic of strong Coulomb interactions, another energy scale—the discrete energy levels due to electron confinement—emerges as temperature decreases, and it modifies the tunneling spectra. Unlike the case of a two-junction configuration, where the electrons are confined by the two contacts if the nanotube is clean enough, in a single-junction configuration the electrons can be confined by disorders when the MWNTs are "dirty," such that the impedance of the local environment of the junction is larger than R_Q. A stacking mismatch between adjacent walls and other structural imperfections are possible sources of disorders in MWNTs, resulting in discrete energy levels.

By cooling down the devices to below 1 K, we observe that G develops a narrow resonancelike anomaly at very low bias (Fig. 3). The asymmetric anomaly builds up consistently as temperature decreases and even shows a dip structure. The line shape resembles that of a Fano resonance.

Unlike the Coulomb structure, which is caused by static e-e interaction, a Fano resonance is a manifestation of quantum interference of two scattering channels: a discrete energy level and a continuum band. It has recently been rediscovered in mesoscopic systems such as semiconductor quantum dots [16,17]. Taking a quantum dot as an example, it can be considered as a gate-confined droplet of electrons with localized states. The coupling of

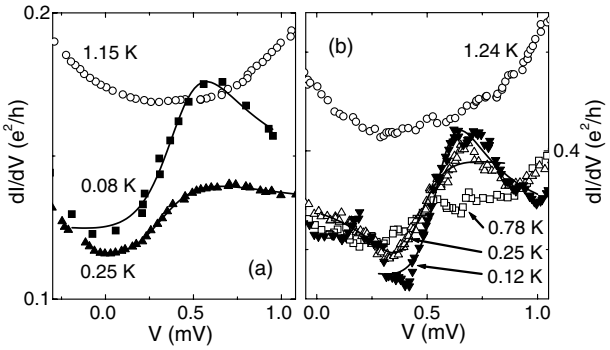

FIG. 3. Asymmetric resonance features of dI/dV seen in two samples: 990530s1 (a) and 990530s6 (b). The lines are the fits of Fano's formula. Fitting parameters are listed in Table II.

the dot to the leads can be tuned to control the system to enter different transport regimes: If the dot is weakly coupled with the environment, a well-established CB develops. The charge transport is suppressed except for narrow resonances at charge degeneracy points. When the tunnel barriers become more transparent, the dot enters the Kondo regime—i.e., below a characteristic Kondo temperature T_K, spin-flip cotunneling events introduce a narrow symmetric TDOS peak at E_F that can be interpreted as a discrete level. If the coupling is strong enough, the interference between this discrete level and the conduction continuum gives rise to an asymmetric Fano resonance. In Ref. [16], such a crossover from a well-established CB through a Kondo regime to a Fano regime has been clearly observed.

We find that the asymmetric resonance curve of G can be fitted by the Fano's formula: $G = G_{\text{inc}} + G_0(\epsilon + q)^2/(\epsilon^2 + 1)$. Here G_{inc} stands for the incoherent background conductance, q is the so-called asymmetry parameter, $\epsilon = (eV - \varepsilon_0)/(\gamma/2)$ is the dimensionless detuning from resonance, and γ is the FWHM of the resonance. As expected, the asymmetric parameter q, which is a measure of the degree of coupling between the discrete state and the continuum, increases when the temperature drops (see Table II).

The Kondo temperature, estimated from the relation $\gamma = 2k_B T_K$, is consistent for each device at different temperatures and agrees with the observed FWHM of the resonance. If Kondo physics truly exists, then G at voltages near the resonance should show nonmonotonic temperature dependence around T_K [18]. Indeed, the G-V

TABLE II. Characteristics of the two samples in Fig. 3.

Sample	T (K)	q	ε_0 (meV)	γ (meV)	T_K (K)
990530s6	0.25	0.53	0.43	0.32	1.86
990530s6	0.12	1.75	0.57	0.29	1.68
990530s1	0.25	0.92	0.3	0.65	3.77
990530s1	0.08	1.97	0.43	0.56	3.25

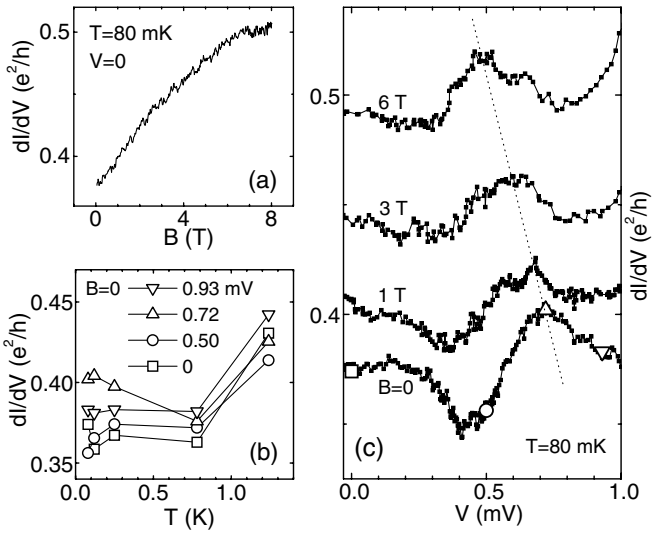

FIG. 4. (a) The dependence of zero bias dI/dV on perpendicular magnetic field. (b) The temperature dependence of dI/dV measured at different voltages. (c) Effect of perpendicular magnetic field. From bottom to top: $B = 0$, 1, 3, 6 T (sample 990530s6). The evolution of the conductance peak is highlighted by the dashed line.

curves in Fig. 3 exhibit such behavior: G at the peak position first drops with T and then rises up below $\sim$1 K [plotted in Fig. 4(b)]. Moreover, we find that a perpendicular magnetic field gives rise to effects that are twofold [Figs. 4(a) and 4(c)]: First, the background conductance increases monotonically with the applied magnetic field. Second, the dip seen at zero field gradually disappears and the resonance turns into a nearly symmetric peak at high field, similar to the pattern observed in semiconductor quantum dots [16].

The magnetic field effect can be explained as follows: First, adding a flux should change the amplitude and/or the phase for the resonant channels and therefore break down the coherent backscattering and increase the forward transmission through the channel. Second, the magnetic field can destroy the interference between the resonant and nonresonant paths, transforming a resonant dip into a peak.

Since Kondo physics is historically interpreted as the interplay between the d orbitals of magnetic impurities and the conduction continuum, we have to eliminate the possibility that the observed Fano resonance comes from residual traces of the Fe/Si catalyst in the MWNT samples. It has been shown that magnetic impurities in MWNTs cause an enhancement of thermoelectric power [19], which is absent in our careful thermoelectric power measurements [20]. Furthermore, no Fe signature can be detected in the body of the MWNT bundles within the instrumental resolution in the energy dispersion x-ray and TEM studies. Therefore, similar to the Kondo effect in the CB regime which has been studied theoretically [21,22] and observed experimentally [18,23], the Fano resonance observed here must also be an inherent property of MWNTs, which can be virtually treated as quantum dots strongly coupled to the leads.

In summary, strong zero-bias suppression of the TDOS is observed in MWNTs' single tunnel junctions that can be explained well by the EQF theory. The observed exponent $\alpha \approx 0.25$–0.35 is found to be consistent for all the samples. Similar to the case of an open quantum dot, in low-impedance junctions we find that a Fano-resonance-like asymmetric conductance anomaly builds up below mV energy scales. It seems that MWNTs provide us a good laboratory to study the interplay between strong e-e interaction and disorder scattering.

The authors acknowledge fruitful discussions with R. Egger, M. Bockrath, W. Zheng, T. Xiang, G. M. Zhang, and Y. P. Wang. This work is supported by the National Key Project for Basic Research, the Knowledge Innovation Program of CAS, and the NSFC.

*Present address: Gordon McKay Laboratory of Applied Science, Harvard University, MA 02138, USA.

[1] M. Bockrath *et al.*, Nature (London) **397**, 598 (1999).
[2] L. Langer *et al.*, Phys. Rev. Lett. **76**, 479 (1996).
[3] A. Bachtold *et al.*, Nature (London) **397**, 673 (1999).
[4] J. Haruyama, I. Takesue, and Y. Sato, Appl. Phys. Lett. **77**, 2891 (2000).
[5] A. Bachtold *et al.*, Phys. Rev. Lett. **87**, 166801 (2001).
[6] R. Tarkiainen *et al.*, Phys. Rev. B **64**, 195412 (2001).
[7] G.-L. Ingold and Y.V. Nazarov, in *Single Charge Tunneling*, edited by H. Grabert and M. H. Devoret, NATO ASI, Ser. B, Vol. 294 (Plenum, New York, 1991).
[8] Z.W. Pan *et al.*, Nature (London) **394**, 631 (1998).
[9] When superconductors such as Sn are used as the metal strip, an additional suppression in dI/dV is seen below T_c in zero magnetic field, which proves that the electron transport is via a tunneling process.
[10] G.-L. Ingold and H. Grabert, Europhys. Lett. **14**, 371 (1991).
[11] W. Zheng *et al.*, Solid State Commun. **108**, 839 (1998).
[12] For a recent review, please see J. J. Lin and J. P. Bird, J. Phys. Condens. Matter **14**, R501 (2002).
[13] N. Kang *et al.*, Phys. Rev. B **66**, 241403(R) (2002).
[14] R. Egger and A. O. Gogolin, Phys. Rev. Lett. **87**, 066401 (2001); Chem. Phys. **281**, 447 (2002).
[15] E. G. Mishchenko, A.V. Andreev, and L. I. Glazman, Phys. Rev. Lett. **87**, 246801 (2001).
[16] J. Gores *et al.*, Phys. Rev. B **62**, 2188 (2000).
[17] W. G. van der Wiel *et al.*, Science **289**, 2105 (2000).
[18] J. Nygard, D. H. Cobden, and P. E. Lindelof, Nature (London) **408**, 342 (2000).
[19] L. Grigorian *et al.*, Phys. Rev. B **60**, R11 309 (1999).
[20] N. Kang *et al.*, Phys. Rev. B **67**, 033404 (2003).
[21] L. I. Glazman and M. E. Raikh, JETP Lett. **47**, 452 (1988).
[22] T. K. Ng and P. A. Lee, Phys. Rev. Lett. **61**, 1768 (1988).
[23] M. R. Buitelaar *et al.*, Phys. Rev. Lett. **88**, 156801 (2002).